Interrelation Between Preparation Conditions, Structure, and Mechanical Reinforcement in Isoprene Rubber Filled with *In Situ* Generated Silica

F. Bignotti,[1] S. Borsacchi,[2] R. de Santis,[1] M. Geppi,[2,3] M. Messori,[4] U. P. Sudhakaran[2]

[1]*Dipartimento di Ingegneria Meccanica e Industriale, Università degli Studi di Brescia, Via Branze 38, 25123 Brescia, Italy*
[2]*Dipartimento di Chimica e Chimica Industriale, Università di Pisa, Via Risorgimento 35, 56126 Pisa, Italy*
[3]*Consorzio Interuniversitario Nazionale per la Scienza e Tecnologia dei Materiali, INSTM, Via G. Giusti 9, 50121 Firenze, Italy*
[4]*Dipartimento di Ingegneria dei Materiali e dell'Ambiente, Università degli Studi di Modena e Reggio Emilia, Via Vignolese 905/A, 41125 Modena, Italy*

Received 8 August 2011; accepted 20 September 2011
DOI 10.1002/app.36337
Published online 20 January 2012 in Wiley Online Library (wileyonlinelibrary.com).

ABSTRACT: The sol–gel technique was used to reinforce isoprene rubber (IR) by generating silica *in situ* from tetraethoxysilane (TEOS). The aim of the research was to elucidate the effect of the preparation conditions on the structural and morphological characteristics of silica and the resulting mechanical reinforcement. The structure of the *in situ* generated silica was analyzed by ^{29}Si high-resolution solid-state NMR spectroscopy, which evidenced a high condensation degree of TEOS that decreased with increasing the sol–gel reaction time. The silica dispersion became less homogeneous as the TEOS content and the reaction time were increased. The incorporation of a coupling agent (OTES, octyltriethoxysilane) in the reaction mixture promoted full conversion of TEOS. Lower particle size, better silica dispersion, and higher filler-matrix adhesion were noticed if the incorporation of OTES was delayed compared to TEOS. Uniaxial tensile tests evidenced that the tensile strength typically increased in the first 60 min of reaction and then leveled off. A similar behavior was observed for the high deformation stiffness, whereas at low deformations, the stiffness increased monotonically with the reaction time. In the vulcanizates with silica contents higher than 25 wt %, a drastic stiffness decrement was observed passing from low to high deformations. This reduction was ascribed to the disruption of the secondary filler network occurring in these materials when severely stretched. © 2012 Wiley Periodicals, Inc. J Appl Polym Sci 125: E398–E412, 2012

Key words: elastomers; electron microscopy; mechanical properties; NMR; silicas

INTRODUCTION

Elastomers generally require the incorporation of reinforcing fillers to enhance their basic properties and make them useful for commercial applications. Carbon black and silica are the most used fillers for the reinforcement of rubber compounds. In general, silica provides a better combination of tear strength, abrasion resistance, and aging resistance compared to carbon black.[1] Furthermore, in the tire industry, silica imparts to tire treads a lower rolling resistance than carbon black at equal wear resistance and wet grip.[2] However, the presence of polar hydroxyl groups on the silica surface induces in conventional nonpolar elastomers particle aggregation and poor dispersion, which results in a decrement of the mechanical properties. Furthermore, the incorporation of silica into elastomers by mechanical mixing requires long mixing times at elevated temperatures and therefore high power consumption. Among the various strategies devised to circumvent the above problems, the most popular is the reduction of silica surface polarity by treatment with silane coupling agents, which, however, are expensive and can interfere with the vulcanization process.[3]

A recently developed method to obtain silica-reinforced rubbers is based on the sol-gel process, where a liquid silica precursor, typically tetraethoxysilane (TEOS), previously incorporated in the rubber, generates silica particles *in situ*, that is, directly in the rubber matrix. During the sol–gel process, as a result of the hydrolysis of TEOS ethoxysilane (—Si—OC_2H_5) groups, silanol (—Si—OH) groups are first formed, which then react with other ethoxysilane or silanol groups and form siloxane (Si—O—Si) linkages through condensation reactions, in which water or ethanol (EtOH) is eliminated.[4–6] The use of

Correspondence to: F. Bignotti (fabio.bignotti@ing.unibs.it).

TABLE I
Nominal and Actual Silica Content and Conversion of TEOS to Silica (C_{TEOS}) of the Prepared Filled Rubber Samples

Sample	Nominal silica content		Actual silica content		C_{TEOS} (%)
	phr	wt %	phr	wt %	
IRV_30_0	30	23.1	10.9	9.8	36.3
IRV_30_30	30	23.1	16.1	13.9	53.7
IRV_30_60	30	23.1	17.9	15.2	59.7
IRV_30_180	30	23.1	23.9	19.3	79.7
IRV_50_0	50	33.3	9.6	8.7	19.2
IRV_50_30	50	33.3	34.5	25.6	69.0
IRV_50_60	50	33.3	39.0	28.0	78.0
IRV_50_180	50	33.3	43.0	30.1	86.0
IRV_70_0	70	41.2	14.3	12.5	20.4
IRV_70_30	70	41.2	48.2	32.5	68.8
IRV_70_60	70	41.2	49.7	33.1	71.0
IRV_70_180	70	41.2	49.5	33.1	70.7
IRV_30_0_0	30	23.1	14.7	12.8	49.0
IRV_30_0_30	30	23.1	22.6	18.4	75.3
IRV_30_0_60	30	23.1	22.9	18.7	76.3
IRV_30_0_180	30	23.1	29.9	23.0	99.7
IRV_30_30_30	30	23.1	15.1	13.1	50.3
IRV_30_30_60	30	23.1	17.8	15.1	59.3
IRV_30_30_180	30	23.1	27.7	21.7	92.3

TEOS to prepare silica-filled elastomers was reported for several polymers, including butadiene rubber,[7,8] acrylonitrile-butadiene rubber,[9] styrene-butadiene rubber,[10,11] natural rubber,[8,12–14] isoprene rubber (IR),[15,16] epoxidized natural rubber,[10,17] silicone rubber,[18,19] and thermoplastic elastomers.[20,21]

It is generally accepted that the extent of mechanical reinforcement of elastomers is controlled by (a) the dispersion state of the filler, (b) filler–matrix interactions, and (c) filler–filler interactions.[22–24] A major potential of the sol–gel technique stems from the possibility to control the amount of silica generated *in situ* and its morphological characteristics by a proper selection of the reaction conditions (e.g., amount of TEOS, type and amount of catalyst, temperature, and reaction time). Furthermore, it is possible to tailor filler–filler and filler–rubber interactions through the incorporation of silane-coupling agents in the reaction mixture. These compounds carry in their molecule functional groups suitable to improve filler–matrix interactions, thus allowing to obtain a better silica dispersion and a higher mechanical reinforcement.[25,26]

The authors recently presented a study on the *in situ* generation of silica from TEOS into IR.[15] In that case, the water necessary for the conversion of TEOS to silica was simply absorbed from the external environment, without a strict control of stoichiometry. As a result of the restricted diffusion of water from the environment to the reaction mixture, the conversion of TEOS to silica was limited for samples having a high initial content of TEOS. This problem was subsequently overcome by developing a modified procedure in which the stoichiometric amount of water was introduced in the reacting system.[16] In the present work, the latter procedure was followed to prepare a number of IR/SiO_2 vulcanizates with the aim of elucidating the relationships between the preparation conditions, the structural characteristics of the *in situ* generated silica and the resulting mechanical reinforcement. In particular, the effect of the following factors was considered: (a) initial content of TEOS, (b) sol–gel reaction time, and (c) addition to the reaction mixture of octyltriethoxysilane (OTES), a silane-coupling agent. More specifically, three initial TEOS contents were considered, and, for each content, the sol–gel reaction was stopped at different times, and the resulting compound was vulcanized. Thus, three series of IR vulcanizates (IRV) were obtained, which were coded as IRV_30_*z*, IRV_50_*z*, and IRV_70_*z*, where *z* is the reaction time, while 30, 50, and 70 represent the nominal silica contents, that is, the phr of silica expected on the basis of the initial TEOS content, assuming complete conversion of TEOS. For the composition corresponding to 30 phr of silica, two further series were explored, namely IRV_30_0_*z* and IRV_30_30_*z*, which differed for the time of addition of OTES (at 0 or 30 min of the sol–gel reaction time, respectively). Finally, the unfilled IRV was used as a reference material for the assessment of the mechanical reinforcement induced by silica. The complete list of the materials investigated in this work is reported in Table I.

The silica dispersion state was analyzed by scanning electron microscopy (SEM), while ^{29}Si high-resolution solid-state NMR (^{29}Si SSNMR) spectra were used to characterize its chemical structural

properties. Swelling experiments were performed to study the extent of filler-matrix adhesion in the various systems investigated, and, finally, uniaxial tensile tests were carried out to evaluate the mechanical reinforcement induced by silica.

EXPERIMENTAL

Materials

TEOS, OTES, dibutyltin dilaurate (DL), dicumyl peroxide (DCP), ethanol (EtOH), and toluene were purchased from Sigma-Aldrich and used without further purification.

IR with a 97% content of cis units, a viscosity–average molecular mass of $2.3 \cdot 10^6$ g/mol, a glass transition temperature of $-67°C$, and a density of 0.91 g/cm^3 was purchased from Sigma-Aldrich.

Preparation

IR polymer (4 g) was dissolved in toluene (100 mL) at the refluxing temperature, and, after cooling at room temperature, a given amount of TEOS, H_2O, and EtOH (TEOS : H_2O : EtOH = 1 : 4 : 4 molar ratio), DL (2 wt % relative to TEOS as catalyst for the sol-gel process), and DCP (1 wt % relative to IR as vulcanizing agent) were added.

In some cases, OTES (4 wt % relative to IR) was added to mixtures corresponding to a nominal content of silica of 30 phr at the established reaction time, as surfactant/coupling agent. The mixtures usually assumed the aspect of an emulsion because of the presence of a significant amount of water in an organic medium. The mixtures were magnetically stirred and heated at 80°C for different times (up to 3 h) to activate the hydrolytic condensation of TEOS to silica. After the given reaction time, toluene and other volatile products such as H_2O and EtOH were eliminated by using a rotary evaporator operating at reduced pressure and room temperature in order to avoid any significant further progress of the sol–gel reaction in solution.

All the samples were molded into rectangular sheets ($100 \times 50 \times 1.5$ mm^3) and vulcanized at 150°C for 20 min under a pressure of 150 bar by using a hot-plate hydraulic press (Carver).

Silica characterization

The actual silica content in the filled rubber was determined by measuring the weight loss of a sample when combusted to oxidize all organic matter according to ASTM D 5630 Technical Standard (Procedure A. Muffle-Furnace Technique). At least two specimens were tested for each material.

The morphological investigation was carried out by SEM using a Quanta 200 FEI microscope under an accelerating voltage of 15 kV. The sample surfaces (cross section) were coated with gold by an electro-deposition method to impart electrical conduction before recording SEM micrographs.

The density of neat silica, purposely prepared according to the above-reported synthetic conditions from TEOS and DL only, was determined by a pycnometer (AccuPyc 1330 apparatus, Micromeritics, Norcross, GA).

Filled rubber characterization

Solid-state NMR measurements

^{13}C and ^{29}Si high-resolution measurements were performed on a two-channel Varian Infinity Plus 400 spectrometer, operating at 100.59 MHz for carbon-13 and at 79.47 MHz for silicon-29 nuclei, and equipped with a 7.5 mm CP-MAS (Cross Polarization-Magic Angle Spinning) probe, using a ^1H 90° pulse length of 5 μs.

The ^{29}Si CP and direct excitation (DE) MAS spectra were recorded under high-power ^1H-decoupling conditions and at a MAS frequency of 3.5 kHz. For samples with OTES, the spectra were recorded at MAS frequencies of 3.5 and 6 kHz. For CP-MAS spectra, a contact time of 5 ms and a recycle delay of 3.5 s were used and 18,000 transients were recorded. In the case of DE, the ^{29}Si 90° pulse length was 6 μs, a recycle delay of 300 s was used, and 2000 scans were accumulated.

Swelling experiments

Samples $5 \times 5 \times 1.5$ mm^3 in size were immersed in toluene, which was replaced daily with fresh solvent, and after 96 h, their swollen mass m_s was recorded. Toluene was eliminated to determine the dry mass m_d of the samples. The swelling ratio q_w was evaluated from an average of at least three measurements according to eq. (1):

$$q_w = \frac{m_s}{m_d} - 1 \tag{1}$$

Uniaxial tensile tests

Uniaxial tensile tests were performed by an Instron dynamometer (model 3366). The experiments were run at room temperature, on strips $50 \times 5 \times 1.5$ mm^3 in size, using a gage length of 25 mm and a crosshead speed of 10 mm/min. Tensile test data were presented as nominal stress $\sigma_n = F/A_o$ versus elongation $e = \Delta l/l_o$ curves, where F is the applied force and A_o is the initial cross-section area of the

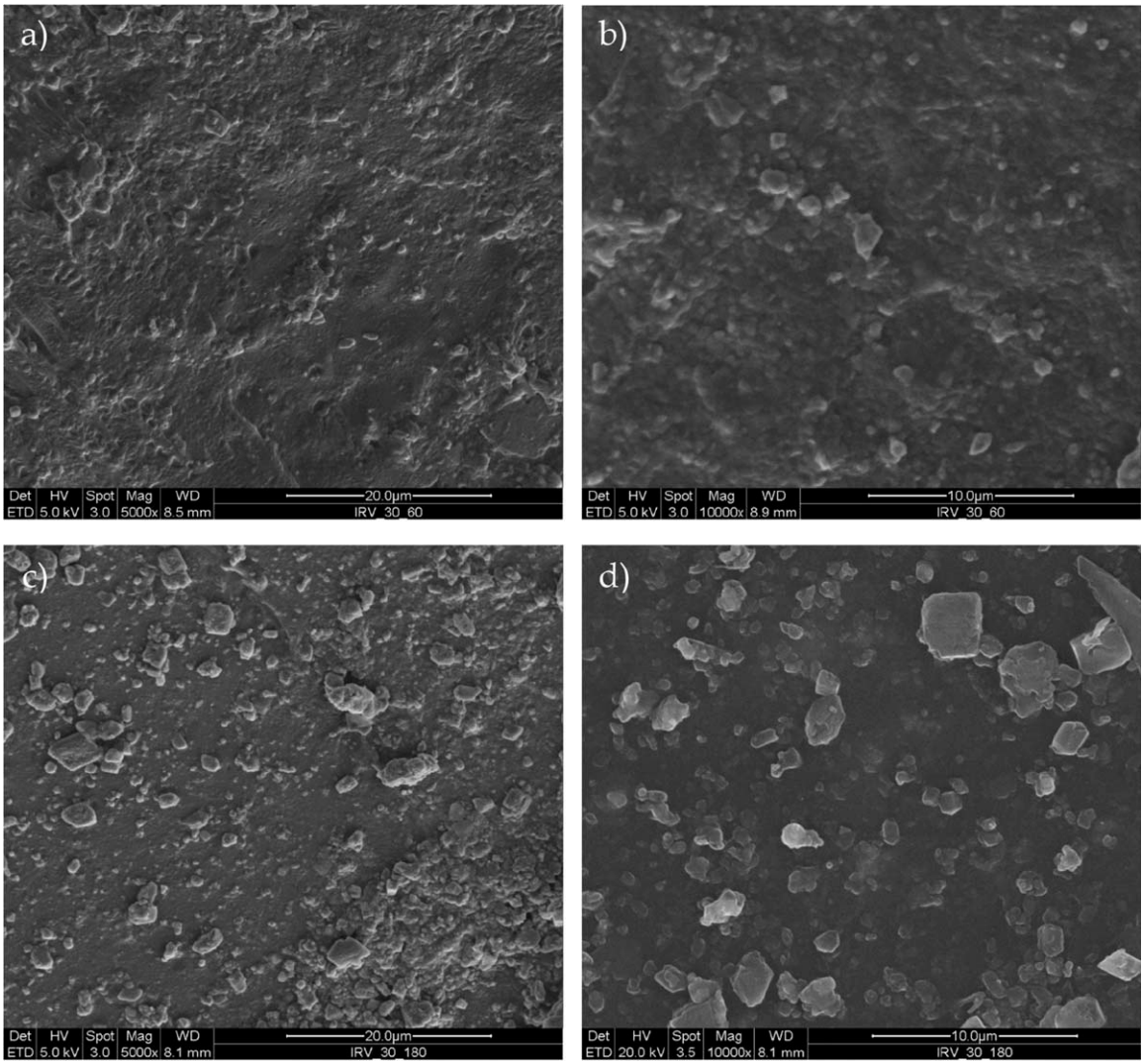

Figure 1 SEM micrographs of a cross-section of IRV_30_60 (a, b) and IRV_30_180 (c, d).

specimen, while Δl and l_o are the change in length and the gage length, respectively. The initial modulus E_{in} was calculated as the slope of the initial portion of the $\sigma_n - e$ curves. The secant modulus at a given elongation $E_{sec,e}$ was calculated as $E_{sec,e} = \sigma_n(e)/e$, where $\sigma_n(e)$ is the nominal stress at the elongation e considered. All mechanical properties were determined on an average of at least four specimens.

RESULTS AND DISCUSSION

Kinetic analysis—Conversion of TEOS to silica

The actual silica content of the prepared filled rubber samples was determined by thermogravimetric measurements, and the values are reported in Table I.

As expected, the actual silica content, correlated with the degree of conversion of TEOS to silica, increased with the sol–gel reaction time, that is, with the time allowed to the mixture to react before it underwent the steps of solvent elimination and rubber vulcanization.

Under the used experimental conditions (time and temperature) for the *in situ* generation of silica within the rubber matrix, IRV_30_*z*, IRV_50_*z*, and IRV_70_*z* showed a good conversion of TEOS to silica even if complete conversion was not reached within the sol–gel reaction times considered (maximum C_{TEOS} = 71–86%). In contrast, actual silica contents very similar to the nominal ones (stoichiometrically calculated by assuming the complete conversion of TEOS to silica) were obtained after a reaction time of 180 min for the rubbers containing OTES, suggesting a non-negligible kinetic acceleration due to the presence of this surfactant/coupling agent.

Finally, it is worth noting that the samples collected after 0 min of sol–gel reaction showed the presence of silica (9–13 wt %) deriving from TEOS

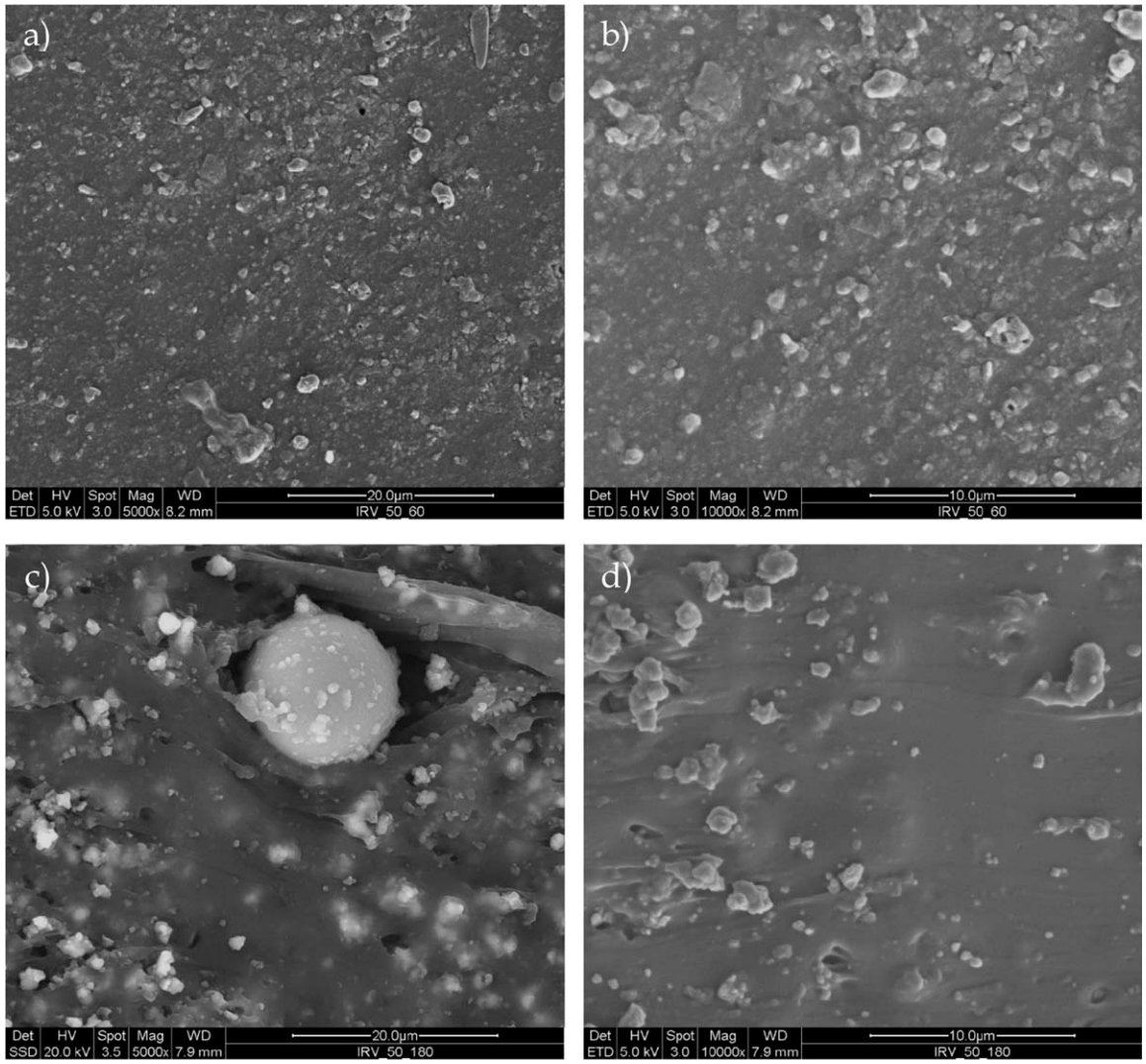

Figure 2 SEM micrographs of a cross-section of IRV_50_60 (a, b) and IRV_50_180 (c, d).

that was converted into silica in the course of rubber vulcanization.

Morphology

Cross-section SEM micrographs of the rubbers obtained with sol–gel reaction times of 60 and 180 min are reported in Figures 1–5. IRV_30_*z* [Fig. 1(a–d)] was characterized by a homogeneous distribution of silica particles within the rubber matrix. The average dimensions increased with the reaction time (diameter values of 1 μm or less for IRV_30_60 and of 3 μm or less for IRV_30_180) presumably due to both the increased conversion of TEOS to silica and to coalescence phenomena of the growing particles.

The distribution of silica particles was still quite homogeneous also in the case of the intermediate initial TEOS content and sol–gel reaction time [IRV_50_60, Fig. 2(a,b)], while a significantly increased inhomogeneity was observed for IRV_50_180 [Fig. 2(c,d)], IRV_70_60 [Fig. 3(a,b)], and IRV_70_180 [Fig. 3(c,d)]. Apart from a worse distribution, some big particles (diameter of 10–30 μm) were observed in IRV_50_180 and IRV_70_180, presumably due to coalescence phenomena, even if the typical diameter of silica particles was actually maintained in the range 1–3 μm or less.

The presence of triethoxysilane groups and octyl groups in the OTES molecules should ensure both the reactivity toward the inorganic phase during the silica particle growth and a good interaction with the organic IR matrix. To verify its effectiveness as surfactant and thus its effect on the final morphology of the hybrids, OTES was added to the reacting mixture at different times (sol–gel reaction times of 0 and 30 min, respectively). Concerning this point, the SEM micrographs reported in Figures 4 and 5 show that the delayed addition of OTES (IRV_30_30_*z* with respect to IRV_30_0_*z*) led to a markedly improved homogeneity with particular concern to

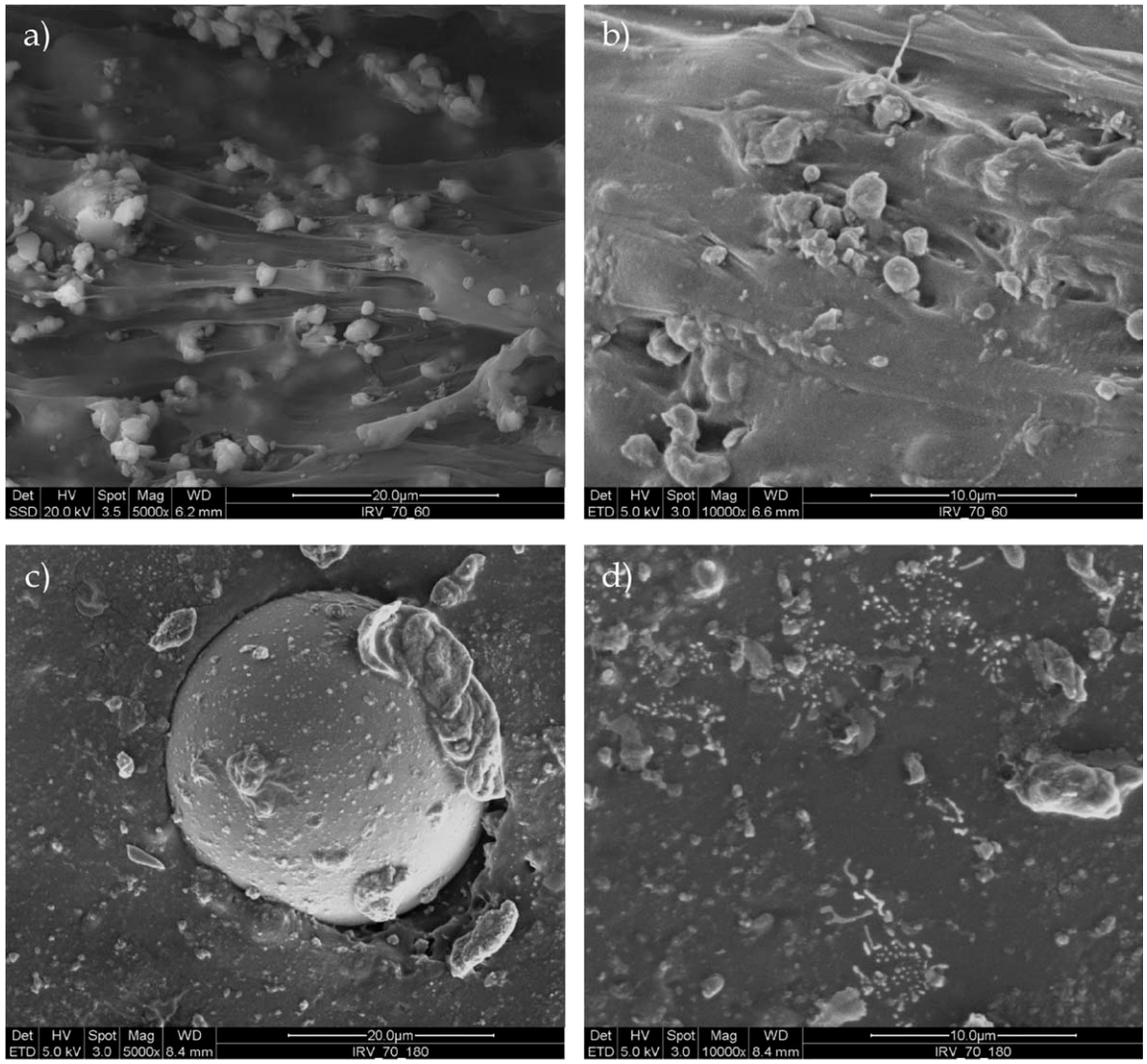

Figure 3 SEM micrographs of a cross-section of IRV_70_60 (a, b) and IRV_70_180 (c, d).

the highest sol–gel reaction time. Indeed, the average size and distribution of silica particles were more or less the same for IRV_30_0_60 and IRV_30_30_60, while after 180 min of sol–gel reaction time a very good distribution uniformity was obtained only in the case of IRV_30_30_180.

It can be speculated that triethoxysilane groups of OTES, if added from the beginning, reacted with TEOS in the early stages of the reaction and octyl groups, remaining "entrapped" in the bulk of the forming inorganic silica network, did not explicate their action as surfactant/coupling agent at the surface of the silica particles. On the contrary, when OTES was added after 30 min to the reacting mixture, that is, after the nucleation and partial growth of the silica particles, smaller and significantly better distributed particles were observed than in IRV_30_0_*z* and IRV_30_*z*. On the basis of this analysis, the addition of OTES after a partial conversion of TEOS (that is after the nucleation of the silica particles) seems to stabilize the surface of the growing particles, acting as an effective surfactant agent to reduce coalescence phenomena.

Structural properties

Solid-state NMR is a very powerful and increasingly used technique for characterizing the structural properties of either organic or inorganic components in organic–inorganic multicomponent materials.[27,28] In the field of elastomer matrix composites, the molecular dynamic properties of filled rubbers have been investigated mainly through the study of ^{1}H–^{1}H dipolar couplings,[29–31] while ^{29}Si high-resolution spectra have been exploited for characterizing the structure of silica and silanes used as filler and compatibilizers (see, for instance, Ref. 32), respectively. Here, we have made extensive use of ^{29}Si

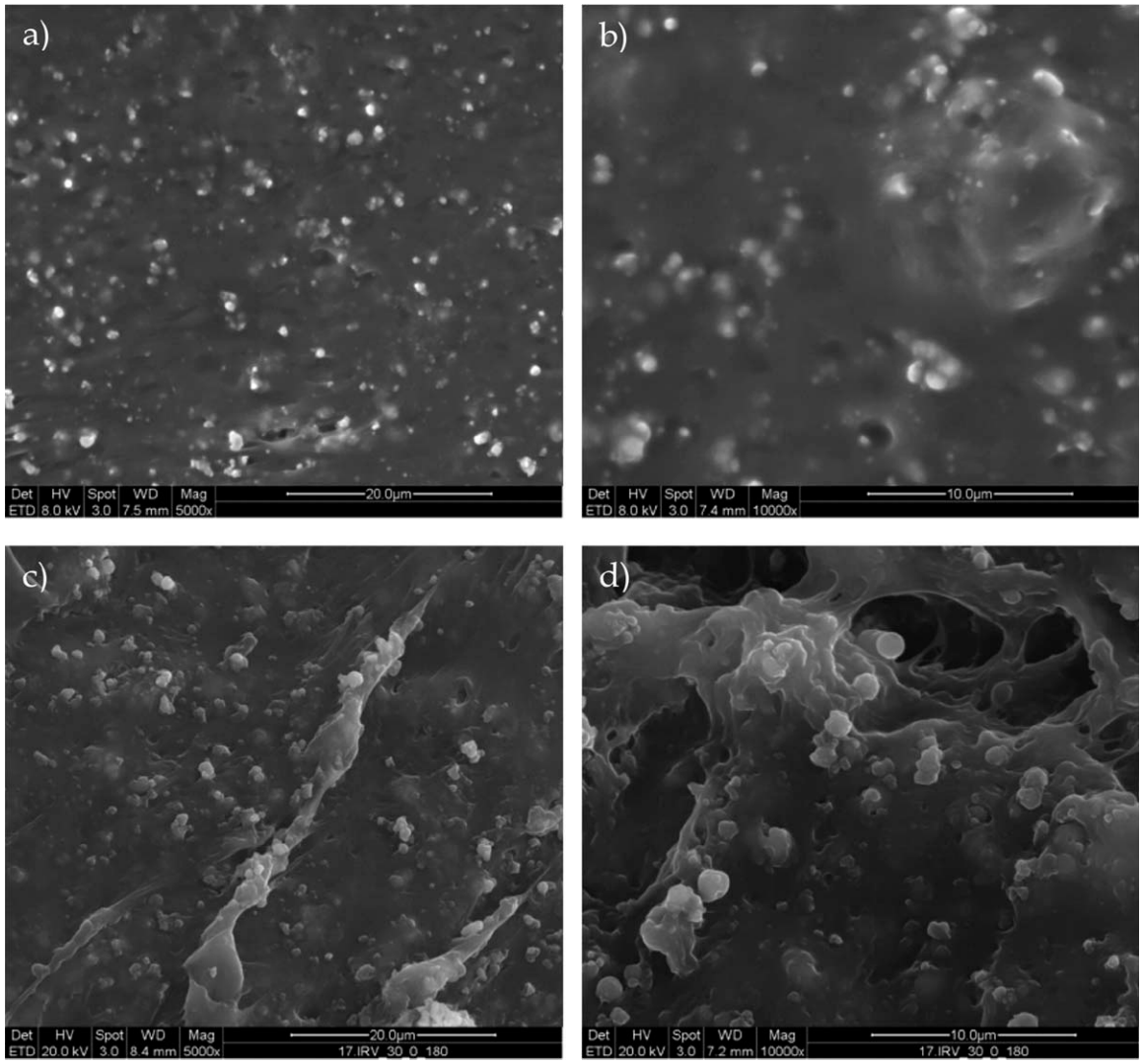

Figure 4 SEM micrographs of a cross-section of IRV_30_0_60 (a, b) and IRV_30_0_180 (c, d).

high-resolution spectra for characterizing the chemical structural properties of the *in situ* generated silica[33–34] and of the added compatibilizer, while a wide characterization of the molecular dynamic properties of the rubber in the hybrids will be the subject of a future publication.

With the aim of characterizing the dependence of the structure of the *in situ* generated silica on the TEOS content as well as its evolution with the sol–gel reaction time, we recorded ^{29}Si CP-MAS spectra of all the filled rubbers [Fig. 6(a–c)]. In all the spectra, three signals can be clearly recognized at −112, −103, and −94 ppm and assigned to fully condensed silicon nuclei (Q^4: ($Si(OSi)_4$)), single silanols (Q^3: ($Si(OSi)_3OH$)), and geminal silanols (Q^2: ($Si(OSi)_2(OH)_2$)), respectively. Indeed, the same signals could also arise from non- or partially hydrolyzed TEOS; however, the presence of ethoxy groups has been ruled out from the ^{13}C CP-MAS spectrum at least for IRV_30_180. Given the dependence of CP signal integrals on contact time, different for silicon nuclei experiencing different ^{1}H-^{29}Si dipolar couplings, CP spectra are intrinsically nonquantitative, being generally favored, in decreasing order, Q^2, Q^3, and Q^4 signals.[35] Nonetheless, because we verified a similar CP dynamics for all samples, the spectra, recorded in the same experimental conditions, can be compared and commented in terms of structural differences among the samples. The first observation concerns the overall integral of the spectra, which is related to the content of silica. It is evident that for IRV_50_*z* and IRV_70_*z*, there is a strong increase of the integral in passing from 0 to 30 min of sol–gel reaction time, while, for longer times, the increase is less pronounced. On the contrary, for IRV_30_*z*, the increase between 0 and 60 min is quite small, and the maximum increase is observed in passing from 60 to 180 min of sol–gel reaction, in qualitative

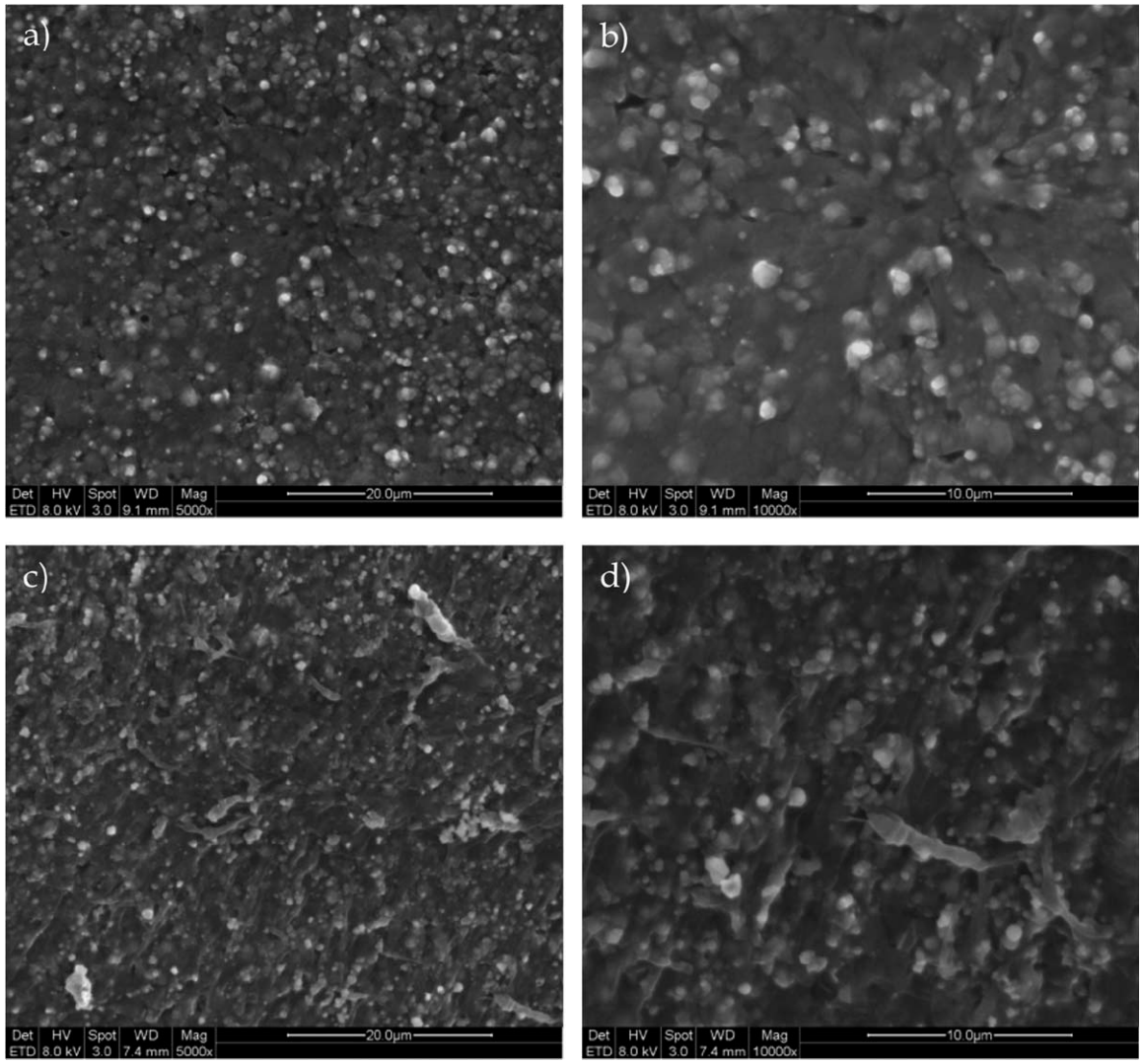

Figure 5 SEM micrographs of a cross-section of IRV_30_30_60 (a, b) and IRV_30_30_180 (c, d).

agreement with composition data reported in Table I, indicating that the kinetics of the reaction is quite strongly related to the TEOS content. Qualitative information on the condensation degree (c.d.) of the formed silica can be obtained looking at the intensity of Q^3 and Q^2 silicon signals with respect to that of Q^4: the most evident result is the increase of the Q^3/Q^4 ratio with increasing the reaction time, which indicates a corresponding decrease of the c.d. of the silica formed. To obtain a quantitative estimate of the silica c.d., a DE ^{29}Si spectrum was recorded on one vulcanizate (IRV_30_180), using a recycle delay between two consecutive transients long enough (300 s) to ensure the quantification of the signal integrals. The DE spectrum clearly shows that fully condensed (Q^4) silicon nuclei are the most abundant species, contrary to what appears from the CP spectrum of the same sample [Fig. 6(d)]. By comparing Q^2, Q^3, and Q^4 signal integrals in the DE spectrum with the corresponding ones in the CP spectrum, both obtained by suitable spectral deconvolutions [see Fig. 6(e)], we could obtain scaling factors that, applied to the signal integrals of the CP spectra of all the samples, allowed us to estimate their corresponding quantitative values (Table II). Then, by using these values, we could estimate the c.d. of silica in all materials, defined by the following equation as the ratio between condensed Si—O—Si groups and total number of Si—O groups:

$$c.d. = \frac{4Q_4 + 3Q_3 + 2Q_2}{4(Q_4 + Q_3 + Q_2)} \quad (2)$$

where Q_i is the integral, in arbitrary units, of the corresponding Q^i signal. The silica c.d. values obtained for the various rubbers analyzed are reported in Table II and plotted versus the sol–gel reaction time in Figure 7. It can be observed that the c.d. is always high (0.915 ÷ 0.946); at almost all the reaction times,

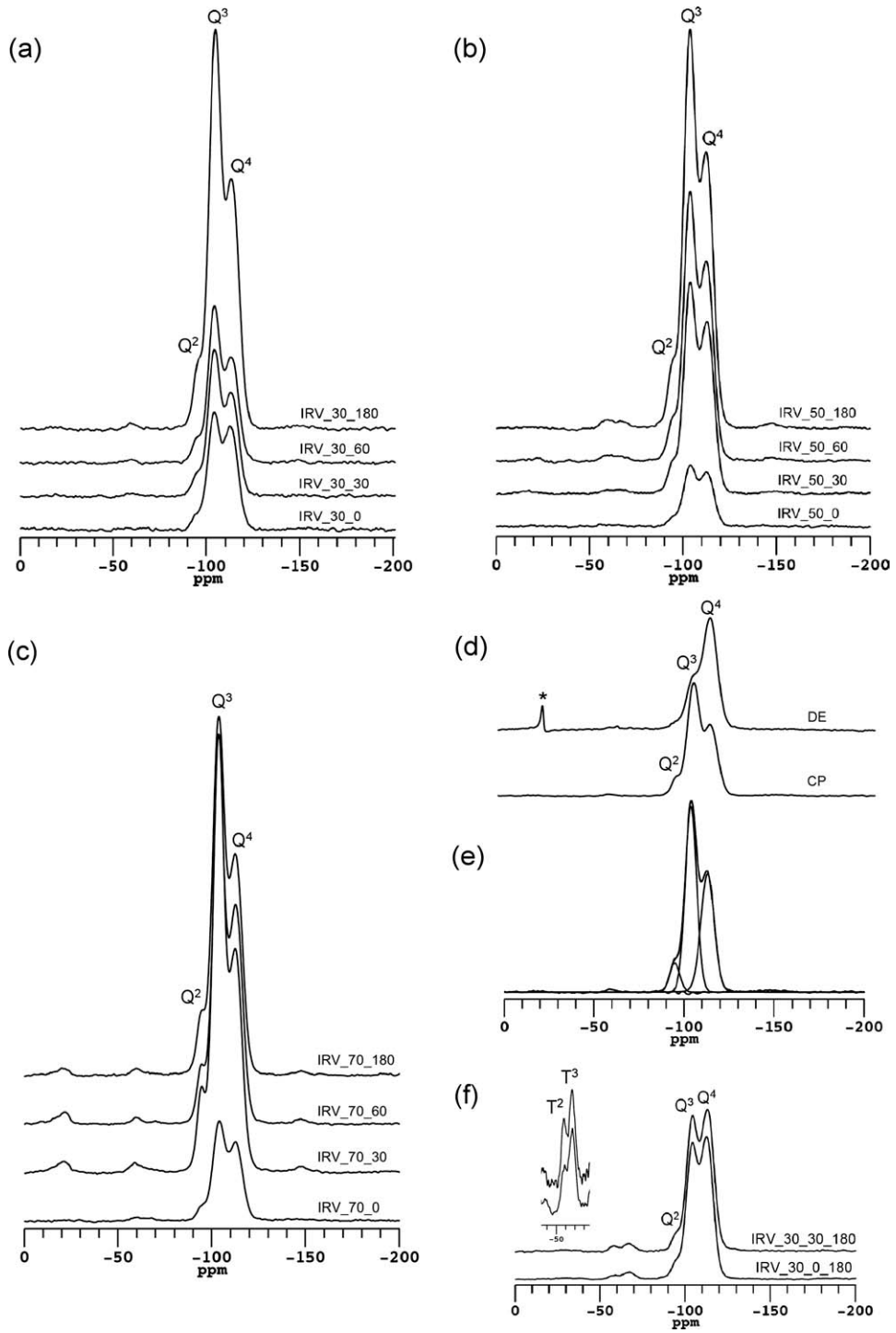

Figure 6 ^{29}Si CP-MAS spectra, acquired at a MAS frequency of 3.5 kHz of (a) IRV_30_*z*; (b) IRV_50_*z*; (c) IRV_70_*z*; small peaks visible at about −60, −70 ppm are spinning sidebands. The signal assignment is reported on the peaks. (d) Comparison between ^{29}Si CP- and quantitative DE-MAS spectra of IRV_30_180. The small peak at about −20 ppm in the DE-MAS spectrum is probably due to impurities of the rubber. (e) Deconvolution of the CP-MAS spectrum of IRV_30_180. (f) ^{29}Si CP-MAS spectra, acquired at a MAS frequency of 6 kHz, of IRV_30_0_180 and IRV_30_30_180; in the inset an expansion of the T silicon signals is shown.

it decreases in passing from IRV_50_*z* to IRV_30_*z* to IRV_70_*z*, and, for all the three series, it tends to decrease with increasing the reaction time. These results empirically suggest that, as a consequence of the complex interplay of the many kinetic and thermodynamic factors involved in the sol–gel processes, the hydrolysis and condensation reactions tend to become more and less favored, respectively, as the reaction time increases. From an alternative standpoint, a larger fraction of silanols becomes sterically

TABLE II
Integrals of the Signals of the Different Silica Silicon Species (Q^i) Obtained from Deconvolutions of ^{29}Si CP-MAS Spectra ("Cross-Polarization" Columns)

	Cross-polarization			Direct-excitation			
Sample	Q^2 (%)	Q^3 (%)	Q^4 (%)	Q^2 (%)	Q^3 (%)	Q^4 (%)	Condensation degree
IRV_30_0	5.0	45.2	49.8	1.6	18.4	80.0	0.946
IRV_30_30	6.5	50.3	43.2	2.2	22.3	75.5	0.933
IRV_30_60	7.0	49.7	43.3	2.4	22.0	75.6	0.933
IRV_30_180	7.3	51.8	40.9	2.6	23.6	73.8	0.928
IRV_50_0	5.9	45.0	49.1	1.9	18.5	79.6	0.944
IRV_50_30	6.0	46.1	47.9	2.0	19.2	78.8	0.942
IRV_50_60	6.7	47.6	45.7	2.2	20.4	77.4	0.938
IRV_50_180	7.4	49.3	43.3	2.6	21.8	75.6	0.933
IRV_70_0	6.0	46.1	47.9	2.0	19.2	78.8	0.942
IRV_70_30	9.3	55.0	35.7	3.6	27.1	69.4	0.915
IRV_70_60	7.3	52.1	40.6	2.6	23.9	73.5	0.927
IRV_70_180	7.5	53.5	39.0	2.8	25.0	72.2	0.924
IRV_30_0_180	6.3	48.3	45.4	2.2	20.7	77.1	0.937
IRV_30_30_180	5.5	45.9	48.6	1.8	18.9	79.3	0.944

In the "Direct Excitation" column, the signal integrals of the quantitative DE-MAS spectrum of IRV_30_180, representing the actual Q^i silicon percentages, are reported. As described in the text, the "Direct Excitation" Q^i values for all the other samples have been calculated by multiplying the Q^i integrals measured in their CP spectra for the corresponding scaling factors Q^i (DE)/Q^i (CP) experimentally obtained for IRV_30_180. In the last column of the table, silica condensation degree values, calculated as defined in eq. (2), have been reported. The experimental uncertanties on Q^i integrals and condensation degree values are ± 0.05 and ± 0.002, respectively.

inaccessible for condensation. Moreover, the compositions of the IRV_50_*z* are the ones ensuring the most efficient c.d. at almost all the reaction times, even though the differences with the other compositions are quite small.

^{29}Si CP-MAS spectra were also recorded for two vulcanizates containing OTES (IRV_30_0_180 and IRV_30_30_180) [Fig. 6(f)]. Signals ascribable to T^3 ($Si(OSi)_3R$) and T^2 ($Si(OSi)_2$ (OX)R, with X=H or CH_2CH_3) OTES silicon nuclei can be observed at −67 and −58 ppm, respectively. Their presence indicates a noticeable degree of condensation for the SiO groups of OTES reacted with silica, which must be probably ascribed also to a partial self-condensation among OTES molecules. The spectra clearly show that OTES condensation is higher when it is added at the beginning of the reaction. By comparing the silica c.d. in these two materials (obtained by applying the above described scaling factors to the Q^i signal integrals in their CP spectra recorded in the same experimental conditions used for all the rubbers without OTES) with that of the corresponding vulcanizate without OTES (IRV_30_180; Table II), it can be observed that the presence of OTES, especially if added after 30 min of the sol–gel reaction, seems to favor the condensation of silica.

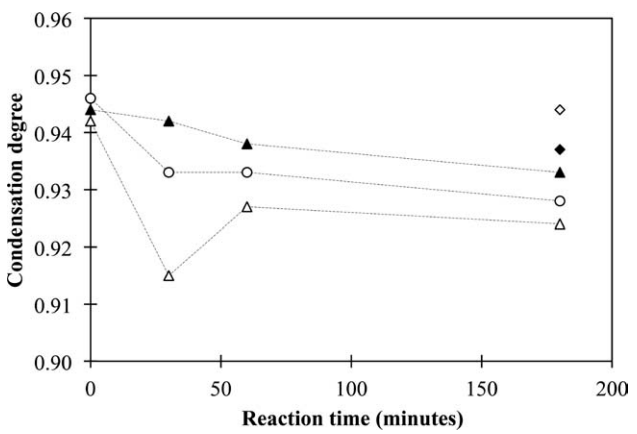

Figure 7 Plot of silica condensation degree versus sol–gel reaction time, as obtained from ^{29}Si SSNMR spectra. Symbols: open circle, IRV_30_*z*; full diamond, IRV_30_0_*z*; open diamond, IRV_30_30_*z*; full triangle, IRV_50_*z*; open triangle, IRV_70_*z*.

Swelling behavior

Swelling experiments were performed to follow the conversion of TEOS to silica and to investigate the extent of filler-matrix adhesion in the various systems investigated. In fact, the solvent absorbed per unit mass of material, that is, the swelling ratio, is expected to decrease with increasing the filler concentration first because silica does not absorb toluene and second because, when good adhesion exists at the rubber-filler interface, nonabsorbing silica particles restrict swelling of the IR network located in proximity of the interface.

In Figure 8, the swelling ratio q_w of the various systems is plotted versus the sol–gel reaction time. In all cases q_w at $t = 0$ is lower than the swelling

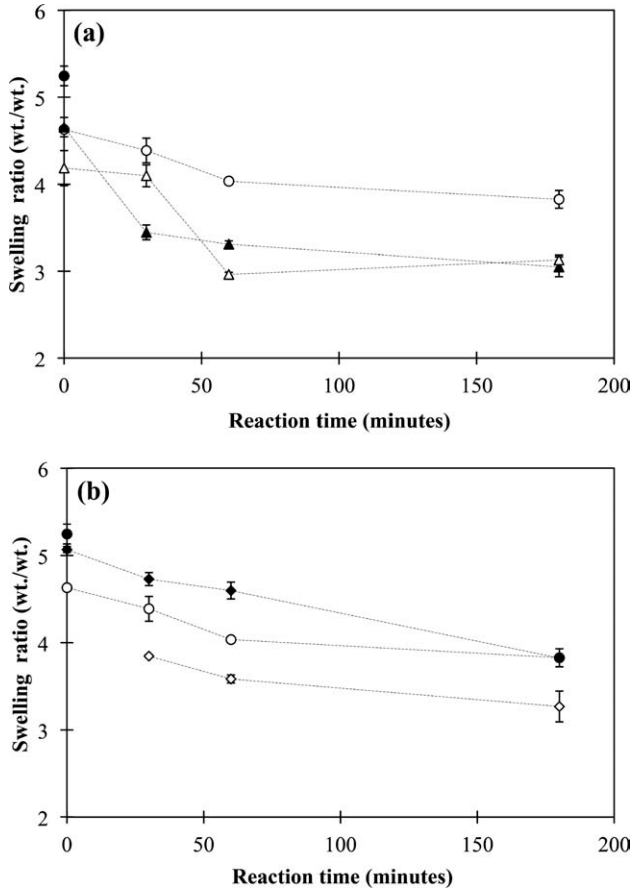

Figure 8 Swelling ratio as a function of the sol–gel reaction time for rubbers prepared in the absence (a) and in the presence (b) of OTES. Symbols: full circle, IRV; open circle, IRV_30_*z*; full diamond, IRV_30_0_*z*; open diamond, IRV_30_30_*z*; full triangle, IRV_50_*z*; open triangle, IRV_70_*z*.

ratio of IRV because of the presence of some silica deriving from a partial conversion of TEOS during the preparation of these materials. As expected, the swelling ratio decreases with time. The drop of q_w follows qualitatively the increase of silica concentration (see Table I), with the exception of IRV_70_30, which has a swelling ratio similar to that of IRV_70_0 but much higher filler content.

An analysis of swelling data according to a model developed by Kraus[36] was carried out to clarify the effect of the reaction parameters on the extent of filler-matrix adhesion. According to this model, if swelling is completely restricted at the rubber-filler interface due to adhesion, the following relation should hold:

$$\frac{V_r^o}{V_r} = 1 - m\frac{\Phi}{1-\Phi} \tag{3}$$

where V_r is the volume fraction of rubber in the swollen filled rubber phase, V_r^o is the same quantity referred to the unfilled vulcanizate, Φ is the volume fraction of filler (in the unswollen state), and m ($m > 0$) is a parameter dependent on V_r^o and on filler characteristics. Thus, if V_r^o/V_r is plotted as a function of $\Phi/1-\Phi$ (Kraus plot), a linear decrease should be observed in the case of good adhesion at the matrix-filler interface. In contrast, the model predicts an increase of V_r^o/V_r with $\Phi/1-\Phi$ when no adhesion exists.

In the present case, V_r, V_r^o, and Φ were calculated from eqs. (4) and (5), which can be obtained under the assumption of volume additivity:

$$V_r = \left[1 + \frac{\rho_r}{\rho_s}\frac{q_w}{\left(1 - \frac{w}{100}\right)}\right]^{-1} \tag{4}$$

$$\Phi = \frac{w\ \rho_r}{\mathrm{w}\ \rho_r + (100 - w)\ \rho_f} \tag{5}$$

where ρ_r (0.93 g/cm^3), ρ_s (0.86 g/cm^3), and ρ_f (1.66 g/cm^3) are the densities of neat rubber, solvent, and filler, respectively, while w is the weight percentage of silica in the rubber (see Table I). The values of ρ_r and ρ_f were determined by measuring, respectively,

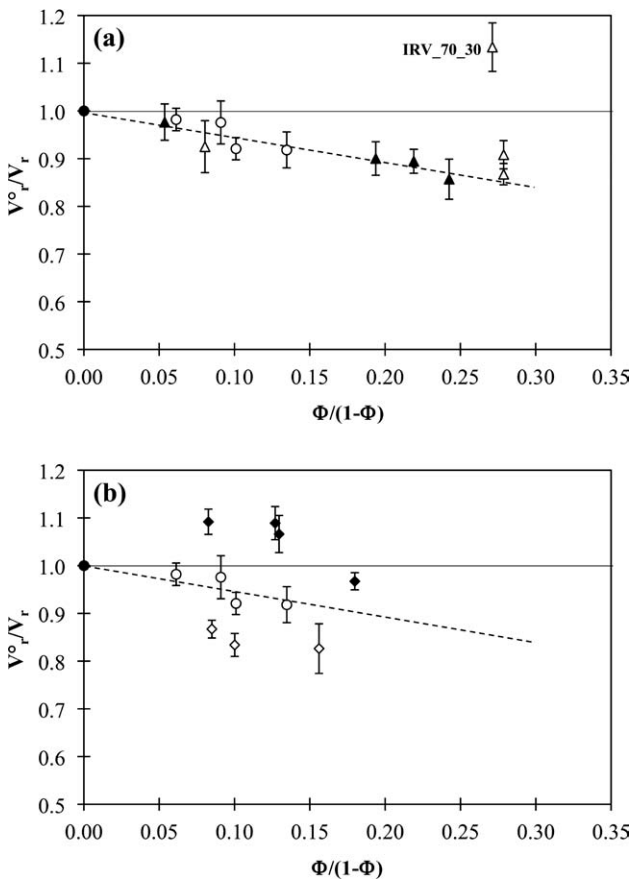

Figure 9 Kraus plot for rubbers prepared in the absence (a) and in the presence (b) of OTES. Symbols: full circle, IRV; open circle, IRV_30_*z*; full diamond, IRV_30_0_*z*; open diamond, IRV_30_30_*z*; full triangle, IRV_50_*z*; open triangle, IRV_70_*z*.

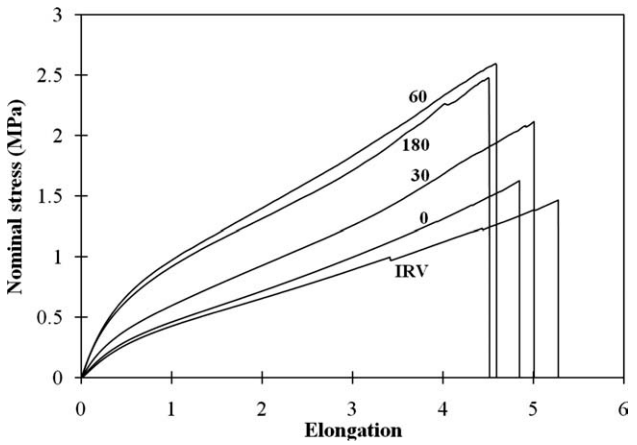

Figure 10 Typical nominal stress versus elongation curves for IRV and IR_50_*z* rubbers (*z* = 0, 30, 60, and 180).

the density of IRV and of silica purposely prepared from TEOS under experimental conditions similar to those used to prepare filled rubbers.

The Kraus plot for rubbers prepared in the absence of OTES is shown in Figure 9(a). Apart from IRV_70_30, V_r^o/V_r is always less than unity, and the experimental points lie approximately along a straight line, as predicted by the Kraus model for adhering fillers. The anomalous behavior of IRV_70_30 might be explained by considering that it is the vulcanizate with the lowest silica c.d. (as estimated from NMR, see Fig. 7) and therefore the highest amount of silanol groups. Thus the relatively high concentration of hydrophilic silanol groups at the interface with the hydrophobic IR matrix might reduce the filler-matrix adhesion.

The effect of OTES on adhesion can be inferred from Figure 9(b). If OTES is incorporated at 30 min of the sol–gel reaction, lower values of V_r^o/V_r are observed compared to IRV_30_*z*, which suggests an enhancement of IR-SiO_2 adhesion. When analyzing adhesion as evaluated from solvent swelling, it should be considered that it is indirectly evaluated from the restriction to matrix swelling in comparison with the unfilled rubber. As a matter of fact, swelling is more severely restricted the stronger are filler–matrix interactions, and the larger is the area of the filler–matrix interface. From Figures 1, 4, and 5, it can be clearly noticed that silica particles in IRV_30_30_*z* are smaller than in IRV_30_*z* and IRV_30_0_*z* rubbers, so that the filler percentage being the same, the area of the IR-SiO_2 interface is larger in IRV_30_30_*z* than in IRV_30_*z* and IRV_30_0_*z*. Thus, the different swelling behavior of IRV_30_*z* and IRV_30_30_*z* can be explained, at least in part, on the basis of their different morphology.

When OTES is added to the reaction mixture along with TEOS (IRV_30_0_*z* materials), values of V_r^o/V_r greater than unity (at least for $t \neq 180$ min) are observed. It is possible that, under these circumstances, OTES is able to reduce the matrix cross-link density. For instance, given its emulsifying action, OTES might favor trapping into the growing silica network of the vulcanizing agent molecules, which would require long reaction times to escape into the rubbery phase and contribute to cross-linking during the subsequent vulcanization step. This would explain why only for the longest reaction time

TABLE III
Mechanical Properties at Room Temperature as Determined from Uniaxial Tensile Tests

Material	E_{in} (MPa)	$E_{sec,e=1}$ (MPa)	e_b (−)	σ_b (MPa)
IRV	0.80 ± 0.14	0.41 ± 0.04	5.8 ± 2.0	1.4 ± 0.3
IRV_30_0	0.91 ± 0.02	0.47 ± 0.02	4.8 ± 0.8	1.7 ± 0.3
IRV_30_30	1.10 ± 0.03	0.58 ± 0.03	4.5 ± 0.1	2.1 ± 0.2
IRV_30_60	1.05 ± 0.06	0.55 ± 0.01	4.7 ± 0.3	2.2 ± 0.2
IRV_30_180	1.35 ± 0.10	0.61 ± 0.03	6.1 ± 0.5	2.5 ± 0.1
IRV_50_0	0.81 ± 0.08	0.45 ± 0.02	4.7 ± 0.7	1.5 ± 0.2
IRV_50_30	1.14 ± 0.10	0.55 ± 0.03	5.1 ± 0.7	2.1 ± 0.2
IRV_50_60	1.90 ± 0.10	0.91 ± 0.11	4.1 ± 0.6	2.6 ± 0.2
IRV_50_180	2.16 ± 0.14	0.90 ± 0.04	4.6 ± 0.2	2.6 ± 0.2
IRV_70_0	1.43 ± 0.03	0.72 ± 0.03	4.3 ± 0.2	2.3 ± 0.2
IRV_70_30	2.18 ± 0.21	0.90 ± 0.03	3.2 ± 0.6	1.8 ± 0.3
IRV_70_60	2.68 ± 0.11	0.86 ± 0.01	4.2 ± 0.6	2.1 ± 0.4
IRV_70_180	3.32 ± 0.41	0.73 ± 0.02	3.9 ± 0.8	1.3 ± 0.2
IRV_30_0_0	0.72 ± 0.06	0.34 ± 0.02	4.7 ± 0.3	1.3 ± 0.1
IRV_30_0_30	1.12 ± 0.10	0.49 ± 0.04	4.8 ± 0.3	2.2 ± 0.3
IRV_30_0_60	1.18 ± 0.10	0.63 ± 0.03	4.4 ± 0.0	2.6 ± 0.1
IRV_30_0_180	1.44 ± 0.16	0.59 ± 0.02	5.5 ± 1.1	2.4 ± 0.4
IRV_30_30_30	0.91 ± 0.09	0.53 ± 0.04	4.0 ± 0.4	1.9 ± 0.1
IRV_30_30_60	1.22 ± 0.08	0.62 ± 0.03	4.1 ± 0.8	2.5 ± 0.3
IRV_30_30_180	1.50 ± 0.20	0.75 ± 0.05	4.3 ± 0.9	2.0 ± 0.2

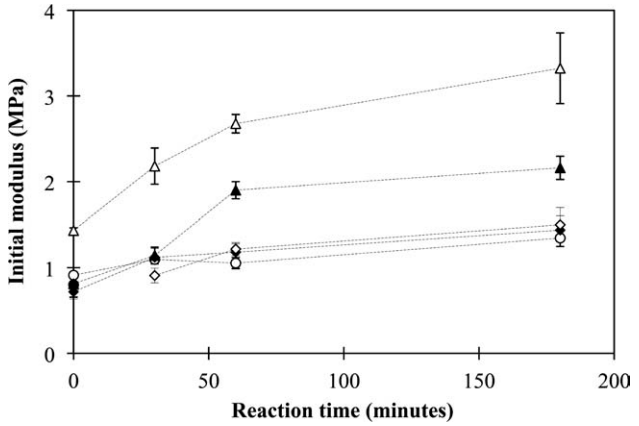

Figure 11 Initial modulus as a function of the sol–gel reaction time. Symbols: full circle, IRV; open circle, IRV_30_*z*; full diamond, IRV_30_0_*z*; open diamond, IRV_30_30_*z*; full triangle, IRV_50_*z*; open triangle, IRV_70_*z*.

analyzed V_r^o/V_r of the IRV_30_0_*z* materials is less than unity.

Mechanical behavior

Uniaxial tensile tests were run on the various materials to investigate the effect of the preparation conditions on the mechanical behavior of the resulting IR/SiO_2 rubbers. The typical effect of the reaction time on the nominal stress (σ_n) versus elongation (e) curves is shown in Figure 10 for the IRV_50_*z* system. With increasing the sol–gel reaction time, and therefore the silica content, the $\sigma_n - e$ curves tend to shift upward due to the reinforcing action exerted by the filler. Similar trends were observed for the other systems investigated, though the variation of the $\sigma_n - e$ curves with the reaction time was different, mainly because of the differences in the conversion rate of TEOS to silica. It is worth noting that the nominal stress versus elongation curves of the materials corresponding to $t = 0$ min were always shifted to higher stresses in comparison with that of IRV because, as already pointed out, these rubbers contained some amount of silica.

From Table III, it can be noticed that the typical values of elongation at break e_b and of stress at break σ_b of filled rubbers are in the range 3–6 and 1.5–2.5 MPa, respectively. As a comparison, for IRV $e_b = 5.8 \pm 2.0$ and $\sigma_b = 1.4 \pm 0.3$ MPa. A general trend for the variation of e_b with the preparation conditions cannot be identified. In contrast, it can be noticed that σ_b usually increases in the first 60 min and then tends to level off. The only exception is IRV_70_*z*, where σ_b decreases with time, probably because, due to progressive coalescence of silica particles, the concentration of coarse particles like that shown in Figure 3 gradually increases with time. Such particles act as stress concentrators, thus reducing the mechanical strength.[37] The leveling of the σ_b values observed in the other series might result from a combination of two factors, namely an increase with time of the average particle size and of the silica content, which have an opposite effect on mechanical strength. As regards the effect of the addition of OTES to the reaction mixture, data of Table III show that it does not appreciably alter the values of the ultimate properties.

The effect of the preparation conditions on material stiffness was analyzed both at very small and at large strains by considering the values of the initial modulus (E_{in}) and of the secant modulus at $e = 1$ ($E_{sec,e=1}$). As highlighted in Figure 11, the initial modulus increases with the reaction time as a consequence of the increment of the silica content. Higher values of E_{in} are obtained at longer times and starting from higher amounts of TEOS. The addition of OTES to the reaction mixture does not exert appreciable effects on the initial modulus. The variation of $E_{sec,e=1}$ with time (Fig. 12) is different, being similar to that pointed out for the mechanical strength: $E_{sec,e=1}$ generally increases in the first 30–60 min and then levels off or, for IRV_70_*z*, decreases. The only exception is IRV_30_30_*z*, where the secant modulus increases steadily with time, so that $E_{sec,e=1}$ is definitely higher in IRV_30_30_180 than in IRV_30_180 or IRV_30_0_180. Therefore, the delayed addition of OTES can improve the large strain stiffness, especially for long reaction times, probably because of the adhesion enhancement evidenced by swelling experiments and the good silica dispersion shown by SEM.

In Figure 13, the values of E_{in} and $E_{sec,e=1}$ are plotted versus the silica volume fraction. Even if some scattering of the experimental data can be noticed, the values of E_{in} for the various systems can be

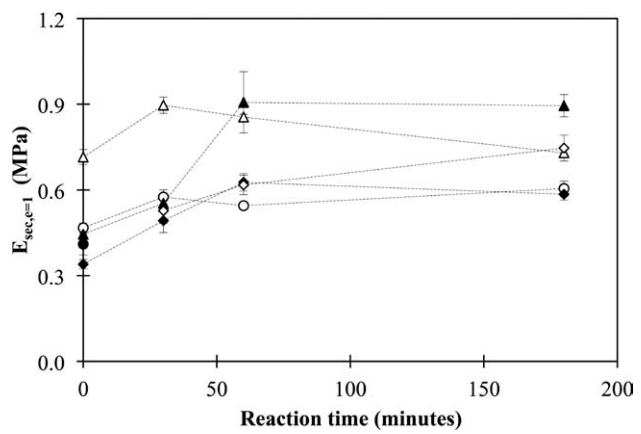

Figure 12 Variation of the secant modulus (elongation = 1) with the sol–gel reaction time. Symbols: full circle, IRV; open circle, IRV_30_*z*; full diamond, IRV_30_0_*z*; open diamond, IRV_30_30_*z*; full triangle, IRV_50_*z*; open triangle, IRV_70_*z*.

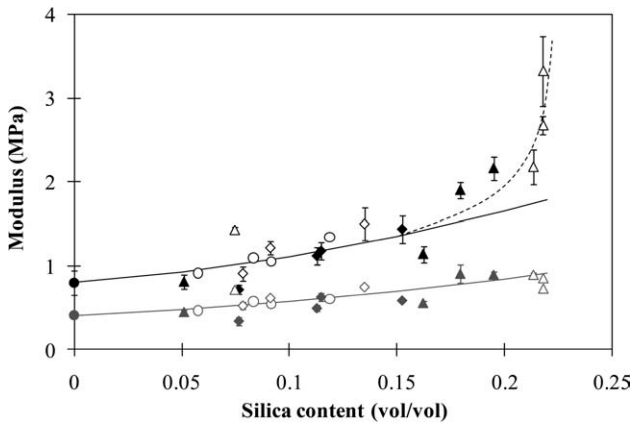

Figure 13 Variation of the initial modulus (black symbols) and of the secant modulus at $e = 1$ (grey symbols) with the silica volume fraction. Continuous curves correspond to the prediction of the Guth equation, in which E_o was taken as the modulus of IRV. The dotted curve was drawn as a guide for the eye. Symbols: full circle, IRV; open circle, IRV_30_*z*; full diamond, IRV_30_0_*z*; open diamond, IRV_30_30_*z*; full triangle, IRV_50_*z*; open triangle, IRV_70_*z*.

described at least approximately by a single curve and the same occurs for $E_{\mathrm{sec},e=1}$. The curves calculated from the Guth equation[38]:

$$E = E_o(1 + 2.5\,\Phi + 14.1\,\Phi^2) \qquad (6)$$

are shown for comparison. In eq. (6), E and E_o are the moduli (initial or secant) of the filled and unfilled rubber, respectively. The Guth equation is useful to predict the modulus of rubbers containing rigid spherical particles. Its validity is limited to low contents, where the filler particles are either isolated or interact pair-wise. At higher concentrations, large deviations from the Guth equation are observed, because, above a critical concentration (percolation threshold), the filler particles form a physical network[39] within the matrix, which causes a considerable raise of modulus in comparison with predictions of eq. (6).

As regards the initial modulus, the Guth equation can fit the experimental data only for $\Phi < 0.16$ (corresponding to $\sim$ 25 wt % of silica), which therefore represents at least approximately the percolation threshold for the systems investigated in this work. In contrast, the secant modulus data follow the prediction of eq. (6) in the whole range of silica contents explored ($0 < \Phi < 0.22$). In addition, it is evident from Figure 13 that for $\Phi > 0.16$, a drastic stiffness reduction occurs passing from low to large strain levels. This behavior resembles the nonlinear dynamic-mechanical behavior typical of filled rubbers, for which the dynamic storage modulus decreases with increasing the strain amplitude (Payne effect).[40] The Payne effect is generally considered as a consequence of the disruption of the filler network under cyclic strain.[41] Therefore, data of Figure 13 suggest that, when the materials with the highest silica contents (IRV_50_60, IRV_50_180, IRV_70_30, IRV_70_60 and IRV_70_180) are in the undeformed state, the filler forms a network that strongly increases the stiffness of these rubbers. When they are stretched to a sufficiently high elongation, the silica network is disrupted, and a remarkable modulus drop takes place. The good fitting of $E_{\mathrm{sec},e=1}$ data obtained with the Guth equation suggests that, for $e = 1$, mainly isolated or pairwise interacting particles are dispersed within the stretched IR matrix.

CONCLUSIONS

^{29}Si SSNMR analysis evidenced for all the preparation conditions considered a high silica c.d., which however decreased with increasing the reaction time, probably because a larger fraction of silanol groups became sterically inaccessible to condensation reactions as TEOS was converted into silica. The SEM analysis showed that the preparation conditions largely affected the silica particle dispersion, which became less homogeneous as the TEOS content and the reaction time were increased. The incorporation of OTES promoted full conversion of TEOS into silica. The effect of OTES on morphology was very much dependent on the time it was incorporated in the reaction mixture. A higher c.d., lower particle size and better filler dispersion were noticed if OTES was added after 30 min of sol–gel reaction. It was suggested that OTES was able to stabilize the surface of the growing particles and reduce the occurrence of coalescence phenomena only if it was incorporated after the nucleation of silica particles, whereas it remained "entrapped" in the bulk of the silica network if it was added at the beginning of the sol–gel reaction.

The application of the Kraus analysis to swelling data highlighted a good filler-matrix adhesion for all vulcanizates, except possibly for those in which OTES was added along with TEOS. The best adhesion was noticed in the vulcanizates prepared by adding OTES after 30 min of reaction. This result was ascribed, at least in part, to the lower particle size and the consequently higher extension of the matrix–filler interface present in these materials.

The tensile tests evidenced that the values of stress at break typically increased in the first 60 min and then tended to level off. This behavior was tentatively related to a combination of two factors, namely an increase with time of the average particle size and of the silica content. As regards the mechanical stiffness, while the variation with time of

the large strain stiffness (secant modulus at the elongation $e = 1$, $E_{sec,e=1}$) was similar to that exhibited by the stress at break, the low-strain mechanical stiffness (initial modulus, E_{in}) increased regularly with the reaction time. The main factor governing the stiffness of the various systems analyzed was the silica content, but, while $E_{sec,e=1}$ increased slowly with the filler concentration, a pronounced increment in E_{in} was noticed for contents higher than 25 wt %. Consequently, in these vulcanizates, a drastic reduction in stiffness was observed passing from low ($e \rightarrow 0$) to high ($e = 1$) elongations. This behavior suggested that the low deformation stiffness of these materials was largely affected by the presence of a secondary filler network, which was disrupted as they were stretched to sufficiently high elongations.

Dr. Elena Fabbri and Ms. Ilaria Puccini are gratefully acknowledged for their support to experimental work.

References

1. Westlinning, H.; Fleischhauer, H. In Reinforcement of Elastomers; Kraus, G., Ed; Wiley:New York, 1965; Chapter 14.
2. Mouri, H.; Akutagawa, K. Rubber Chem Technol 1999, 72, 960.
3. ten Brinke, J. W.; Debnath, S. C.; Reuvekamp, L. A. E. M.; Noordermeer, J. W. M. Compos Sci Technol 2003, 63, 1165.
4. Messori, M. In Recent Advances in Elastomeric Nanocomposites; Mittal, V., Kim J. K., Pal, K., Eds; Springer-Verlag: Berlin Heidelberg, 2011; p 57.
5. Mark, J. E. Polym Eng Sci 1996, 36, 2905.
6. Mark, J. E. Curr Opin Solid State Mater 1999, 4, 565.
7. Sugiya, M.; Terakawa, K.; Miyamoto, Y.; Tomono, S.; Kohjiya, S.; Ikeda, Y. Kautsch Gummi Kunstst 1997, 50, 538.
8. Chung, K. H. J Appl Polym Sci 2008, 108, 3952.
9. Zaborski, M.; Pietrasik, J. Polimery 2002, 47, 643.
10. Kohjiya, S.; Ikeda, Y. Rubber Chem Technol 2000, 73, 534.
11. Yoshikai, K.; Ohsaki, T.; Furukawa, M. J Appl Polym Sci 2002, 85, 2053.
12. Kohjiya, S.; Murakami, K.; Iio S.; Tanahashi, T.; Ikeda, Y. Rubber Chem Technol 2001, 74, 16.
13. Bokobza, L.; Chauvin, J. P. Polymer 2005, 46, 4144.
14. Ikeda, Y.; Poompradub, S.; Morita, Y.; Kohjiya, S. J Sol-Gel Sci Technol 2008, 45, 299.
15. Messori, M.; Bignotti, F.; De Santis, R.; Taurino, R. Polym Int 2009, 58, 880.
16. Messori, M.; Fiorini, M. J Appl Polym Sci 2011, 119, 3422.
17. Bandyopadhyay, A.; De Sarkar, M.; Bhowmick, K. J Mater Sci 2005, 40, 53.
18. Yuan, Q. W.; Mark, J. E. Macromol Chem Phys 1999, 200, 206.
19. Rajan, G. S.; Sur, G. S.; Mark, J. E.; Schaefer, D. W.; Beaucage, G. J Polym Sci Pol Phys 2003, 41, 1897.
20. Lai, S. M.; Liu, S. D. Polym Eng Sci 2007, 47, 77.
21. Huang, Z. H.; Dong, J. H.; Qiu, K. Y.; Wei, Y. J Appl Polym Sci 1997, 66, 853.
22. Yatsuyanagi, F.; Suzuki, N.; Ito, M.; Kaidou, H. Polymer 2001, 42, 9523.
23. Berriot, J.; Martin, F.; Montes, H.; Monnerie, L.; Sotta, P. Polymer 2003, 44, 1437.
24. Fröhlich, J.; Niedermeier, W.; Luginsland, H. D. Compos Part A: Appl Sci Manuf 2005, 36, 449.
25. Tanahashi, H.; Osanai, S.; Shigekuni, M.; Murakami, K.; Ikeda, Y.; Kohjiya, S. Rubber Chem Technol 1998, 71, 38.
26. Tangpasuthadol, V.; Intasiri, A.; Nuntivanich, D.; Niyompanich, N.; Kiatkamjornwong, S. J Appl Polym Sci 2008, 109, 424.
27. Geppi, M.; Borsacchi, S.; Mollica, G. In Encyclopedia of Magnetic Resonance; Harris, R. K., Wasylishen, R. E., Eds.; Wiley: Chichester, 2008.
28. Geppi, M.; Borsacchi, S.; Mollica, G.; Veracini, C. A. Appl Spectrosc Rev 2009, 44, 1.
29. ten Brinke, J. W.; Litvinov, V. M.; Wijnhoven, J. E. G. J.; Noordermeer, J. W. M. Macromolecules 2002, 35, 10026.
30. Litvinov, V. M.; Barthel, H.; Weis, J. Macromolecules 2002, 35, 4356.
31. Dreiss, C. A.; Cosgrove, T.; Benton, N. J.; Kilburn, D.; Alam, M. A.; Schmidt, R. G.; Gordon, G. V. Polymer 2007, 48, 4419.
32. Park, S. J.; Cho, K. S. J Colloid Interf Sci 2003, 267, 86.
33. Geppi, M.; Mollica, G.; Borsacchi, S.; Marini, M.; Toselli, M.; Pilati, F. J Mater Res 2007, 22, 3516.
34. Marini, M.; Toselli, M.; Borsacchi, S.; Mollica, G.; Geppi, M.; Pilati, F. J Polym Sci Polym Chem 2008, 46, 1699.
35. Borsacchi, S.; Geppi, M.; Veracini, C. A.; Fallani, F.; Ricci, L.; Ruggeri, G. J Mater Chem 2006, 16, 4581.
36. Kraus, G. J Appl Polym Sci 1963, 7, 861.
37. Hamed, G. R. Rubber Chem Technol 2000, 73, 524.
38. Guth, E. J Appl Phys 1945, 16, 20.
39. Heinrich, G.; Klüppel, M.; Vilgis, T. A. Curr Opin Solid State Mater 2002, 6, 195.
40. Payne, A. R. J Appl Polym Sci 1962, 6, 57.
41. Heinrich, G.; Klüppel, M. Adv Polym Sci 2002, 160, 1.